Journal Name

ARTICLE

Synthesis and characterisation of lanthanide-hydroporphyrin dyads

Ruisheng Xiong,[a] Julien Andres,[a] Kira Scheffler[a] and K. Eszter Borbas[a]

Fluorescence spectroscopy is in many ways the ideal tool for the interrogation of complex biological systems, as it is non-invasive, sensitive, and offers high spatiotemporal resolution. For biomedical imaging luminescent probes absorbing and emitting in the red-to-near infrared (NIR) region are best suited to maximise tissue penetration and minimise damage to cellular components. NIR-emitting lanthanides (Ln) sensitised with red-absorbing antennae are promising candidates for these applications, assuming the challenges of poor photophysical properties and tedious syntheses of the complexes are overcome. Chlorins are porphyrin-type tetrapyrroles with intense red absorption. Recently chlorins have been shown to sensitise Yb and Nd emission when incorporated into Ln-complexes. Here we expand on our previous work, and explore the effect of chlorin structure, metallation state, chlorin-Ln-complex linker length and mode of attachment on the properties of chlorin-Ln complexes. As chlorin absorption bands are ~20 nm fwhm and readily tunable, a deeper understanding of structure-property relationships would enable the use of chlorin-Ln complexes in multicolour imaging using antenna-specific excitation. A detailed description of antenna and complex syntheses and photophysical characterisation is given. A number of challenges were identified, which will have to be addressed in future studies to enable multicolour imaging using the NIR-emitting lanthanides.

Introduction

The tagging of a large number of species in a straightforward and readily decodable manner is a challenge in chemical biology as well as medical diagnostics.[1] Luminescence is an attractive readout signal for such applications due to its sensitivity and high resolution, and relatively low cost of the instrumentation. Furthermore, luminescence imaging is non-invasive, and is thus well-suited to real-time detection. Lanthanide (Ln) luminescence, consisting of sharp, long-lived emission bands which cover the visible (Tm, Tb, Eu, Dy, Sm) to the near IR (NIR, Yb, Nd and Er) range is increasingly relied on in this area.[2] As Ln intrinsic extinction coefficients are only of a few cm^{-1} M^{-1} their excited state is typically obtained via photosensitisation by organic chromophores. As foremost examples of multicolour imaging, Tb and Eu complexes have been used in FRET-pairs with organic dyes and quantum dots to enable multiplex detection of cancer biomarkers,[3] as well as to study biomolecule interactions.[4, 5] Cocktails of responsive Ln complexes have been used in the two-colour detection of small-molecule analytes,[6] and in the ratiometric detection of enzymes.[7] An advantage of using Ln complexes stems from the chemical similarity of the metals,[8] which provides access to compounds with different functions by a simple exchange of metal centre. This aspect has been beautifully demonstrated by accessing NIR-emitting MOF barcodes by variation of the Ln-mixture composition,[9] and by ICP-MS multiplex analysis of lanthanide-labelled protease substrates[10] and viral DNA.[11] In another example, a pair of complexes with an azaxanthone sensitiser afforded either a red-emitting fluorescent cellular stain (Ln = Eu), or a singlet oxygen-generating photosensitiser (Ln = Tb).[12]

The extension of multicolour imaging to the red and NIR is motivated by the lower levels of background signals in this area, and, for biological applications, the deeper tissue penetration of such light.[13] Because of the inherent low quantum yield of NIR emitting lanthanide complexes, current challenges include limited access to sensitive instrumentation for the detection of NIR-signals, and the dearth of readily manipulated, tunable, strongly absorbing organic fluorophores. The enhanced sensitivity of the Ln-excited states to nearby O-H, N-H and even C-H oscillators can amplify even minor structural differences to a detrimental effect. This has been addressed through ligand deuteration[14-16] and fluorination,[17] as well the application of cage-type Ln-binding motifs[18] instead of the synthetically more tractable macrocyclic units. Nevertheless, tetraazamacrocyclic ligands are most widespread as they are cheap, readily available, and their selective functionalisations are well documented.[19, 20] However, the above-mentioned sensitivity of the Ln-excited states justifies the systematic investigation of different ligand microenvironments created by the macrocycle substituents. Such studies are still relatively rare.

Beyond luminescence applications, Ln^{III}-ions are used in magnetic resonance imaging (Gd),[21, 22] X-ray crystallography (Tb)[23] and biomolecule NMR spectroscopy (Tm, Dy).[24-27] Thus,

the combination of a Gd-complex with a red-absorbing/red-emitting chromophore could provide dual MRI-luminescence bimodal imaging agents in case antenna fluorescence is utilised. One class of suitable red-absorbing chromophores is tetrapyrroles, for example porphyrins and dihydroporphyrins (chlorins).[28, 29] Importantly, porphyrins and chlorins have been shown to sensitise NIR emitting Ln ions,[28-31] and therefore such complexes are potential red-absorbing NIR-emitters. Tetrapyrroles are good singlet oxygen sensitisers for PDT,[32, 33] which suggests that access to theranostic agents for combined MRI-photodynamic therapy should be an option. The excellent Cu-binding of porphyrinic macrocycles has been exploited previously to obtain (^{64}Cu)PET–(Gd)MRI bimodal imaging agents through the combination of ^{64}Cu-porphyrins and 1–4 Gd-DOTA-units.[34, 35] Similar avenues are open for chlorin-Ln dyads, hinting at the potential versatility of these systems.

We have recently reported the synthesis of two sets of Ln-complexes with free base monoaryl, or free base or zinc diaryl chlorin antennae.[36] NIR-emission was observed from several of these complexes upon 337 nm-excitation. Tamiaki and co-workers have reported Yb-emission when sensitised by chlorophyll derivatives.[37] Here we report the synthesis of an extended set of chlorin-equipped Ln-complexes. We have systematically varied the metallation state of the antenna, and the type, length and flexibility of the linker connecting the Ln-binding site to the chlorin. We have performed a detailed photophysical investigation of the antennae in the presence and absence of the lanthanide acceptors, and the preliminary study of the effect of the above factors on the Ln-emission.
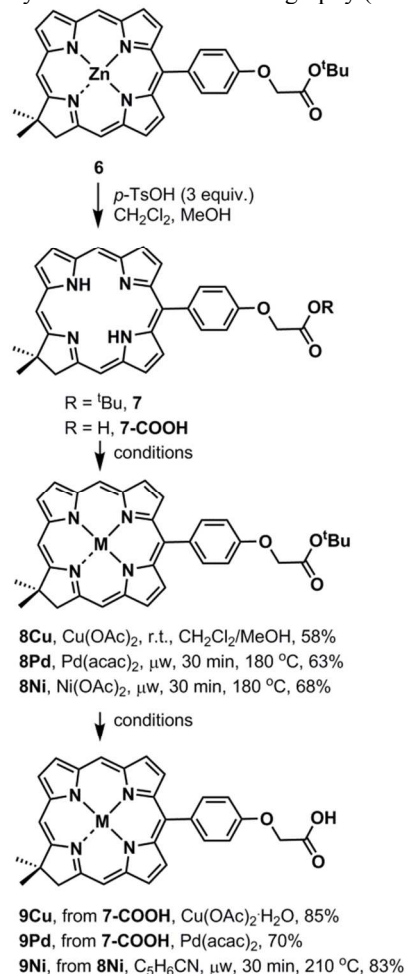
Results and discussion

Synthesis

The synthesis of the chlorin antennae with carboxylate, azide and alkyne reactive groups was based on Lindsey's method.[38, 39] The key step is a one-pot 2+2 macrocyclisation consisting of an acid-catalysed condensation of a tetrahydrodipyrrin (Western half,[40] 4) and a 1-bromo-9-formyldipyrromethane (Eastern half), followed by an oxidative cyclisation under basic conditions. The Eastern halves were synthesised in two steps from aldehydes 1a–d via the corresponding dipyromethanes in moderate to excellent yields (Scheme 1). For the Vilsmeier formylation the use of oxalyl chloride usually gave more consistent results than POCl$_3$, with somewhat higher yields. Bromination of 3a–d to afford 4a–d was quantitative as judged by TLC analysis of the crude products, which were used without further purification. The macrocyclisation affords the zinc chelates of the chlorins. The zinc was retained in the case of the azide, alkyne or TIPS-alkyne-functionalised chlorins. These were destined for Cu-catalyzed azide-alkyne cycloadditions (CuAAC), and the central zinc was a protecting group for the macrocycle. Such a use of zinc metallation is widespread for CuAAC of porphyrins.[41] Preliminary experiments with the free base chlorins also showed that Cu-complexation by the chlorin completely shut down the cycloaddition.
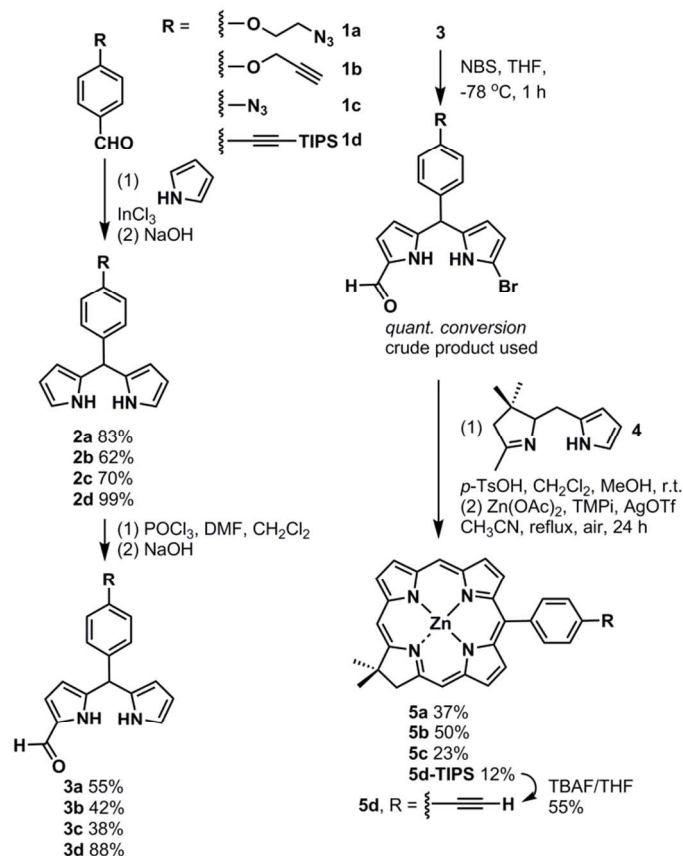
Scheme 1 Synthesis of azide- and alkyne-functionalised chlorin antennae.

In our previous work *tert*-butyl-ester-functionalised chlorin was a key building block,[36] and we prepared Ln-complexes incorporating this motif either as the free base (Yb and Nd) or as the zinc chelate (Nd). Here we wished to gain access to a palette of metallated chlorins in order to study the effect of the central metal on Ln photophysics (Scheme 2). First zinc chelate 6 was demetallated by treatment with *p*-TsOH. Our initial plan was to introduce Cu^{2+}, Pd^{2+} and Ni^{2+} at this stage. Treatment of 7 with Cu(OAc)$_2$·H$_2$O at room temperature, or with Pd(acac)$_2$[42] or Ni(OAc)$_2$·4H$_2$O under microwave irradiation afforded the corresponding chlorins 8Cu, 8Pd or 8Ni in high yield. The relative apolarity of 8Cu, 8Pd and 8Ni enabled the straightforward purification of these chelates. These metallochlorins were expected to be stable to moderately acidic conditions, as previously reported chlorin complexes of these metals were demetallated only under harsh conditions (e.g. concentrated H$_2$SO$_4$/TFA or thiol/TFA).[43, 44] Surprisingly, exposure to even as mild conditions as 10% TFA in CH$_2$Cl$_2$ resulted in significant (in the case of 8Pd almost quantitative) loss of the metal within minutes, making the acidic cleavage of the *tert*-butyl ester unfeasible. It was possible to thermally cleave the ester (8Ni, 210 °C, 30 min, 83%), this method resulted in retention of the metal and essentially no decomposition of the macrocycle. Alternatively, unprotected 7[36] could be metallated. The formation of 9Cu was very straightforward, proceeding at room temperature with complete consumption of starting material within 5 min. The Pd-chelate required much harsher conditions, and typically the use of large excess of Pd(acac)$_2$ with extensive microwave heating was necessary. It was crucial to drive the reaction to completion as the separation of free base and metallochlorins was not possible

under any of the conditions we tried. However, once all free base chlorin was consumed the metal chelates **9Ni** and **9Pd** were readily isolated in analytically pure form in 83–85% yield by silica column chromatography (MeOH:CH_2Cl_2 = 1:10).

6

p-TsOH (3 equiv.)
CH_2Cl_2, MeOH

R = ^{t}Bu, **7**
R = H, **7-COOH**

conditions

8Cu, Cu(OAc)$_2$, r.t., CH_2Cl_2/MeOH, 58%
8Pd, Pd(acac)$_2$, μw, 30 min, 180 °C, 63%
8Ni, Ni(OAc)$_2$, μw, 30 min, 180 °C, 68%

conditions

9Cu, from **7-COOH**, Cu(OAc)$_2$·H$_2$O, 85%
9Pd, from **7-COOH**, Pd(acac)$_2$, 70%
9Ni, from **8Ni**, C$_5$H$_6$CN, μw, 30 min, 210 °C, 83%

Scheme 2 Synthesis of metallated chlorin carboxylic acids.

With the functionalised chlorins in hand we attempted the synthesis of chlorin-lanthanide dyads by reaction with the cyclen-based building blocks shown in Chart 1. Previously we connected chlorin carboxylic acids to amine-carrying cyclen derivatives using HATU as the coupling agent with DIPEA in DMF.[36] These conditions were readily applicable to the new substrates. After ~48 h complete consumption of the chlorins was seen by TLC-analysis of the reaction mixtures. The coupling products were isolated in high yields (65–93%) by aqueous-organic work-up, followed by column chromatography on silica gel. When the cyclen ligand with *tert*-butyl ester groups was coupled to **9Ni** the reaction was slower. Addition of a second portion of reagents to the reaction mixture resulted in complete consumption of starting chlorin, and the product (**13Ni-^{t}Bu**) was isolated in 80% yield.

10

Ln = Yb, **11Yb**
Nd, **11Nd**
Gd, **11Gd**

Ln = Yb, **12Yb**
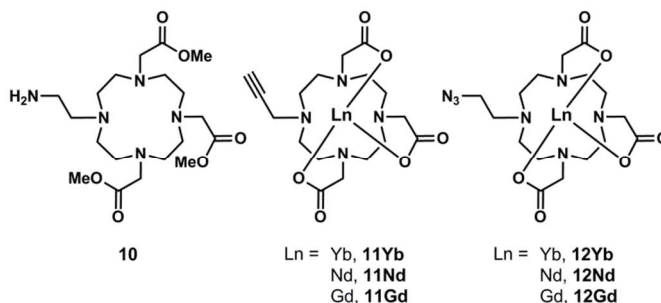Nd, **12Nd**
Gd, **12Gd**

Chart 1

Ligand deprotections and lanthanide complexations were followed by RP-HPLC. Hydrolysis of the methyl esters was surprisingly difficult. Treatment of a solution of **13Pd**, **13Ni** or **13Cu** in CH_2Cl_2/MeOH with a 4-fold excess of NaOH dissolved in MeOH/H_2O resulted in only partial hydrolysis even after 1 week of heating at 60 °C. By RP-HPLC-analysis a mixture was observed, with two major components. We were not able to unambiguously assign the two peaks, however, ^{1}H NMR analysis of the crude reaction mixture suggested the presence of unhydrolysed methyl esters. Addition of first LiOH (10 equiv.), and then KOH (10 equiv.) resulted in the formation of a single compound in all cases. The yield of the hydrolysis is poor after chromatographic purification of the products (~25%). We attempted the thermolysis of **13Ni-^{t}Bu** to the triacid by microwave heating in pyridine at 225 °C. However, these conditions resulted in unacceptably high levels of decomposition, and were abandoned.

Complexations of the lanthanides with the ligands **14**, **14Ni**, and **14Pd** were performed in MeOH at 70 °C in the presence of the appropriate chloride salts. Upon completion of the reaction **15NiLn** precipitated out. Surprisingly, unlike the other Ln-complexes, **15PdLn** was very apolar, and it could be purified by extracting it into CH_2Cl_2. There was a marked difference between the rate of Ln-complexation, with **15NiLn** forming within minutes, **15PdLn** requiring several hours to complete, and the free base **15Ln** proceeding to only ~50% conversion in several days.
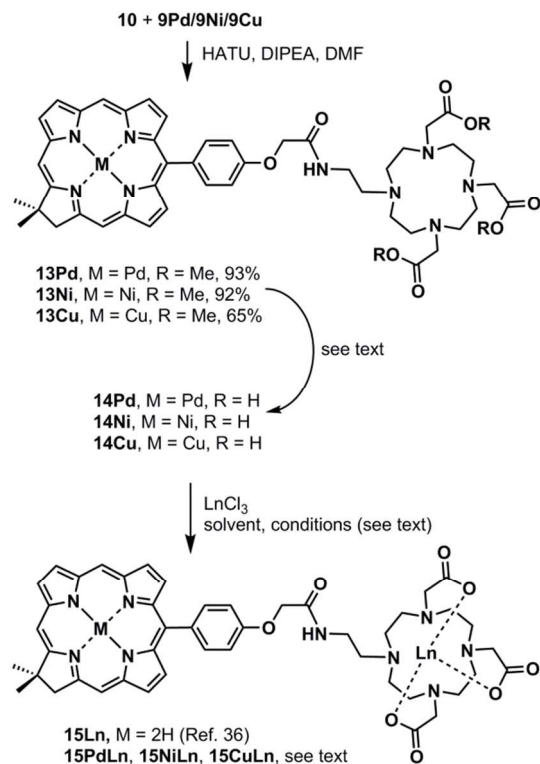
Scheme 3 Formation of the metallochlorin-appended lanthanide complexes.

Scheme 4 Cycloaddition between azidochlorin and alkynyl lanthanide complexes.

Chlorin-appended Ln-complexes were also prepared using Cu-catalysed azide-alkyne cycloadditions between azide- or alkyne-functionalised chlorins **5a–d** and Ln-complexes **10Ln** and **11Ln** bearing complementary reactive groups (Schemes 4 and 5). This way we were hoping to vary the length of the linker, its rigidity, as well as the reactivity profiles of the coupling partners. Despite the successful application of CuAAC in a myriad different settings,[45] its use for Ln-complex functionalisation is not problem-free. Reactions reported to date are often sluggish,[46, 47] low-yielding,[6] or limited in scope due to the harshness of reaction conditions.[48] The complexity of reactions mixtures combined with the low solubility of Ln complexes makes purifications tedious. Nevertheless, where appropriate conditions were identified, often products with interesting properties - to which the trizole bridge was integral - were obtained.[49]

CuAAC between **5a** and **11Ln** progressed smoothly in the presence of CuOAc/NaAsc as Cu[I]-source and TBTA[50] as ligand. The use of DMSO was important to get a homogeneous solution, which in turn appears to be crucial for an efficient reaction of these substrates. We reacted **5b** with **12Ln**, and **5d** with **12Ln** under similar conditions to obtain **ZnNTLn** and **ZnTNLn**, respectively. The reaction between **5c** and **11Ln** returned only starting material both under these conditions, and those reported previously for a range of Ln-complexes (CuI, piperidine:CH$_3$CN, microwave heating).[48] Purification of CuAAC-products was performed as follows. The reaction mixture was concentrated under vacuum, and the residue was dissolved in MeOH. Et$_2$O was added, yielding a dark green precipitate, which was collected by centrifugation. The precipitation procedure was repeated until a solid was obtained that was pure by RP-HPLC analysis. We were not able to obtain analytically pure **ZnNTNd** and **ZnTNLa** this way.
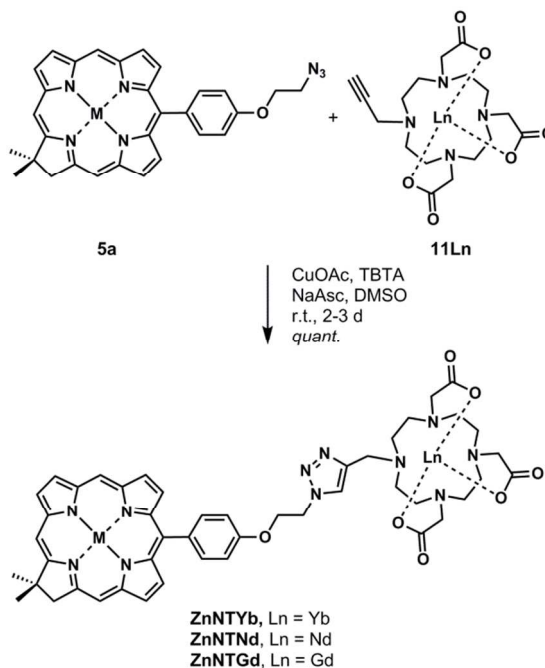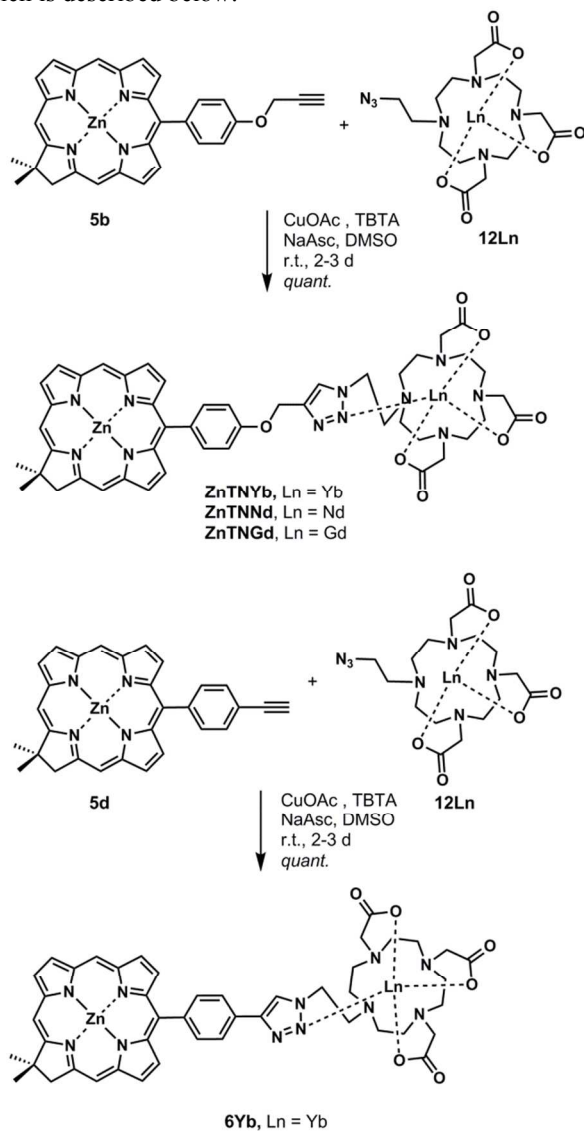
Chemical characterization

All diamagnetic compounds were characterised using standad ^{1}H and ^{13}C NMR and FT-IR spectroscopy, and HR-ESI-MS. In all cases the data were in accordance with the expected structures. Some of the (formyl)dipyrromethane derivatives, the zinc chlorins **5c** and **5d-TIPS** were difficult to purify. For the latter, cleavage of the TIPS group, or demetallation to the free base chlorins afforded readily purifiable compounds. Attachment of the chlorins to the protected cyclen derivatives afforded compounds with complex NMR-spectra, as typical for such species. The identity and the purity of these compounds could be ascertained using a combination of 1D and 2D ^{1}H NMR spectroscopies, HR-MS and RP-HPLC. The hydrolysis of the methyl esters in **13Pd**, **13Ni** and **13Cu** was sluggish even under harsh conditions, and the products were isolated in small quantities. The low solubility of the products (**14Ni**, **14Pd** and **14Cu**), and the paramagnetic nature of the latter precluded the recording of good quality ^{1}H and ^{13}C NMR spectra. We were able to prepare **14Cu** independently from **13**, which is a fully characterised intermediate, by treatment of a solution of **13** in CH$_2$Cl$_2$/MeOH with 1 equiv. Cu(OAc)$_2$·H$_2$O. Addition of the metal salt to the ligand solution resulted in an immediate colour change from dark green to blue. UV-Vis absorption spectroscopy revealed the instantaneous disappearance of the Q-band characteristic of the free base chlorin (λ_{max} = 632 nm), and the appearance of the one typical of the Cu-species (λ_{max} = 596 nm). It seems that metallation of the chlorin proceeds much faster than Cu-binding to the cyclen unit, and selectivity is easily achieved. This material was used as an RP-HPLC reference compound during the hydrolysis of **13Pd**, **13Ni** and **13Cu**. This experiment also suggests that chlorin cupration is a viable reaction for the late-stage radiolabelling of chlorin-containing compounds.

The paramagnetic compounds, i.e. all Cu-chelates, as well Gd-, Yb- and Nd-complexes were characterised by a combination of HR-ESI-MS or MALDI-MS, RP-HPLC and FT-IR. These complexes and the others containing a chlorin

unit were also subjected to photophysical characterisation, which is described below.

Scheme 5 Cycloaddition between alkynyl chlorins and azido lanthanide complex.

Photophysical characterisation

A photophysical characterisation of the chlorin antennae without the appended lanthanide moiety (chlorin reference compounds 6–8) was first undertaken. It was then extended to chlorin-lanthanide dyads attached by a series of linkers. Finally, the ability of the chlorin chromophores to sensitise the NIR emitting lanthanide ions was also investigated.

The specific and interesting photophysical features of porphyrin derivatives are their very high extinction coefficients, large Stokes shifts and their ability to sensitise oxygen to produce reactive singlet oxygen.[32, 51] The photophysical properties of porphyrins can be rationalised by a four orbitals representation (Gouterman orbitals, two HOMOs and two LUMOs).[51, 52] The most intense absorption peaks are located in the blue and are known as the B-band or Soret band. Weaker absorption bands (Q-bands) are found in the green to red region, giving porphyrins and chlorins their characteristic red and green colours, respectively.

Porphyrin-type structures have notoriously poor solubilities, and tend to aggregate. The chlorin reference compounds 6–8 were soluble in MeOH, DMSO, THF and toluene. The free base (7) crystallised overnight from MeOH at concentrations higher than 0.1 mM. This crystallisation was not observed in solutions of the metallated chlorins 6 and 8. In order to compare the chlorin references with our previous results,[36] when solubility permitted the measurements were carried out in methanol. The measurements of 7 were also undertaken in DMSO, yielding bathochromic shifts of the peaks and concentration dependent modifications of the extinction coefficients (see ESI, Figures S1 and S2). The linearity range of the Beer-Lambert law was assessed for 6–8, and good linearity was found in all cases up to $5 \cdot 10^{-6}$ M. At higher concentrations, deviations become more and more apparent, especially for the Zn chlorin 6 (see ESI).

Table 1. Absorption properties of the chlorin reference compounds in methanol. Minimal error due to weight, volume and measurement inaccuracies given in brackets.

	B-Band λ_{max} / nm	ε_B / M$^{-1} \cdot$cm^{-1}	Q-Band λ_{max} / nm	ε_Q / M$^{-1} \cdot$cm^{-1}	$I_B / I_Q{}^a$
7(2H)	401	$1.3(3) \cdot 10^5$	632	$2.6(6) \cdot 10^4$	3.9
6(Zn)	404	$2.5(6) \cdot 10^5$	602	$4(1) \cdot 10^4$	6.0
8Cu	397	$2.7(6) \cdot 10^5$	596	$5(2) \cdot 10^4$	5.4
8Ni	395	$1.3(3) \cdot 10^5$	595	$3.8(9) \cdot 10^4$	3.3
8Pd	390	$1.7(4) \cdot 10^5$	583	$7(2) \cdot 10^4$	2.5

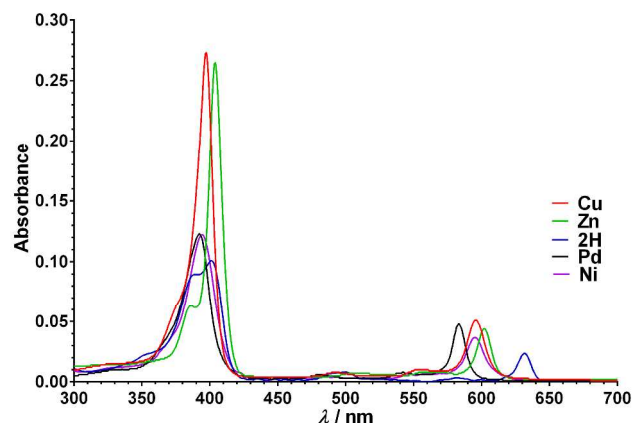^{a} Ratio calculated from the absorbances at a concentration of 1 μM

Figure 1 Absorption spectra of the chlorin reference compounds 6–8 in MeOH (1 μM, 1 cm pathlength).

Absorption properties of 6–8 are presented in Table 1 and **Error! Reference source not found.**. The decadic molar extinction coefficients for the Soret band and Q-band were calculated by averaging the values obtained from the MeOH solutions at concentrations of 0.1 μM, 0.5 μM, 1 μM and 5 μM (linearity range of the absorbance, see ESI, Figure S3). They show an increase of the absorption compared to the free base in the order 2H ≤ Ni < Pd < Zn < Cu. Nevertheless, error calculations (taking into account the error on the mass and volume used to prepare the solutions, as well as the error on the absorbance measurements) showed that some of these extinction coefficients could be quite similar. The well-known hypsochromic shifts upon complexation of porphyrin-type molecules with metallic ions can be observed when comparing the chlorin free base (13) reference compounds 7 with the Zn

(**6**), Cu (**8Cu**), Ni (**8Ni**) and Pd (**8Pd**) complexes. The Soret band is shifted from 408 nm for the free base to 392 nm for the Pd complex, whereas the Q-band is shifted from 634 nm to 583 nm. The Q-band is therefore more affected by the presence of the metal than the B-band.

In order to keep the absorbance as low as possible but still obtain a decent signal, the emission photophysical properties of the chlorin reference compounds were measured at a concentration of 1 μM. This concentration was also used to calculate the I_B/I_Q ratio, the lower concentrations having a larger relative error on the absorbances, which is illustrated by plotting the I_B/I_Q ratio as a function of the concentration (see ESI, Figure S4).
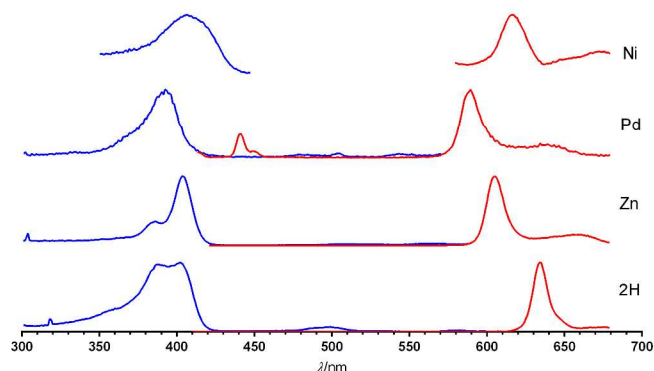

Figure 2 Emission (red) and excitation (blue) spectra of the emissive chlorin reference compounds **6** (Zn), **7** (2H), **13Cu**, **13Pd** and **13Ni**, 1 μM in methanol at room temperature.

The emission and excitation spectra of compounds **6-8** are shown in **Error! Reference source not found.**. The fluorescence bands are located between 589 nm (**8Pd**) and 635 nm (free base **7**). The Ni chlorin had a very low emission, and required that the monochromators be set at high apertures, which yields significant broadening of the emission bands. The excitation spectra overlap quite well with the absorption spectra.

The fluorescence quantum yields of the chlorins were calculated relative to tetraphenylporphyrin (TPP, see a discussion on the choice of standard in the Supporting Information). Free base chlorin **6** exhibited the highest quantum yield of the series with 23%, with 8.4% obtained for Zn chlorin **7**, and 0.05% for **8Pd**. The fluorescence emission of **8Ni** was too weak for the quantum yield to be measured accurately, and finally, **8Cu** was completely non-emissive. These values are typical for free base and metallated chlorins.[53]

The quenching of the emission by Cu was as expected. The low fluorescence quantum yield of the Pd chlorin was also anticipated because of the increased intersystem crossing rate (and thus more pronounced phosphorescence) that should occur with such a heavy ion. This last point seems to be confirmed by low temperature phosphorescence measurements. At 77 K, chlorin phosphorescence from **8Pd** was observed at 760 nm (**Error! Reference source not found.**), whereas the fluorescence was completely extinguished. All the other chlorins retained their fluorescence emission at low temperature, but their phosphorescence was too far in the NIR to be observed with our setup. The lifetime of the triplet state of the Pd chlorin obtained by monoexponential fit of the phosphorescent emission decay was 365 μs.
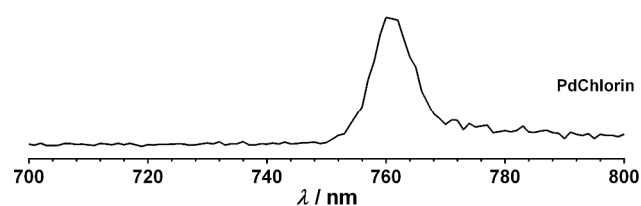

Figure 3. Phosphorescence of **13Pd** at 77 K in MeOH.

The photophysical properties of these chlorin compounds are promising for singlet oxygen production and for the sensitisation of NIR-emitting lanthanide ions. However, when a Ln-do3a moiety is grafted on the chlorin chromophore, the solubility changes drastically. The lanthanide complexes are no longer soluble in methanol and are only poorly soluble in water. Complexes with increased solubility would thus be highly desirable.[54]

Saturated solutions were prepared by allowing solid chlorin-Ln-complexes to stand in water overnight. 10% of THF was then added, but no significant improvement of the solubility was observed. The solutions were then filtered and the filtrate was diluted in water to obtain comparable absorbances for all complexes. Because of this solubility issue, no extinction coefficients could be estimated. The absorbances were thus normalised to highlight the differences in their absorption structures (**Error! Reference source not found.**).
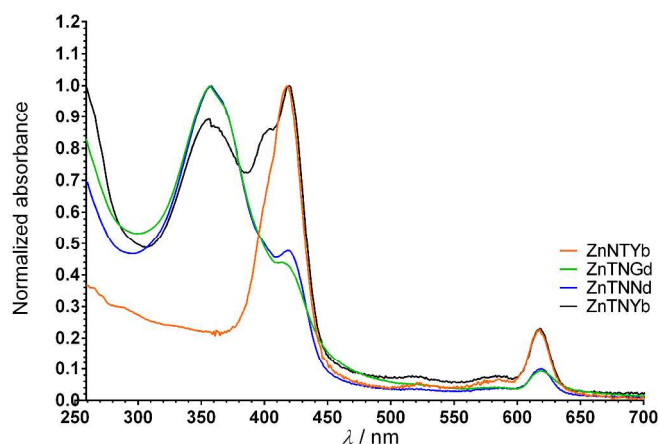

Figure 4. Normalised absorbances of chlorin-appended lanthanide complexes in H_2O, diluted saturated solutions.

The shape of the absorption spectra was quite different for the same Zn chlorin core with different lanthanide ions in the do3a moiety attached to the chlorin chromophore via the same triazole linker (**Error! Reference source not found.**). While the spectra of the Gd and Nd complexes were very similar, the B-band of the Yb complex was very different. The maximum of the Soret band of the Gd and Nd is a broad band around 349 nm whereas the Yb has a normal peak around 409 nm. The broad band is also present in the Yb complex, and has a slightly lower extinction than the peak at 409 nm. The peak at 409 nm appears on the spectra of the Gd and Nd complexes as a shoulder of the 349 nm broad band. Moreover, the Yb complex with the reversed clicked linker is completely different, with absorption features similar to those of the Zn chlorin reference compound. The Q-band is at the same energy (609 nm) for all these complexes.

Because of the poor solubility of the complexes, these changes of the absorption spectra may be due to different types of aggregates. The broadened, red-shifted bands compared to the chlorin reference compound also support aggregation. If so, the reversed clicked linker could help limit aggregation by recovering solubilised species that are closer to the chlorin reference compound.
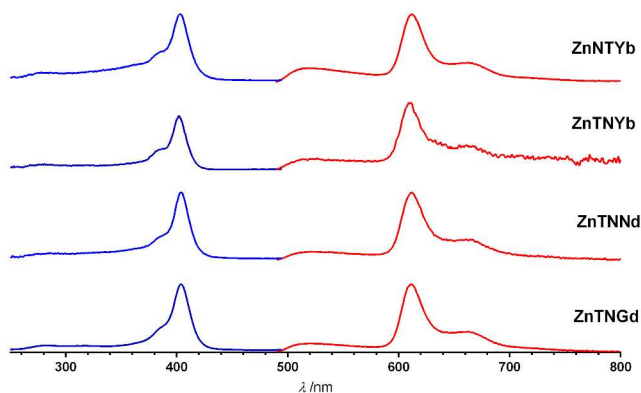

Figure 5. Emission (red) and excitation (blue) spectra of triazole-linked complexes in water.

The fluorescence of Zn chlorin clicked lanthanide do3a complexes is similar irrespective of the lanthanide ion or the triazole linker geometry (Figure 5). The fluorescence quantum yields were estimated relative to TPP. Scattering due to aggregation complicates the comparison of the sample absorption with the reference standard. These quantum yields are therefore to be taken with caution. We calculated $\Phi_f = 0.5\%$ for **ZnNTGd** and **ZnNTYb**, 0.23% for **ZnNTNd** and 0.08% for the reversed clicked linker **ZnTNYb**. Despite all precautions, the reversed linker seems once more to behave differently and yields a lower fluorescence quantum yield. We could not find evidence that this lower quantum yield is correlated with an increased luminescence from the Yb ion since our setup was not able to measure NIR emission.

Finally, we tried to investigate the NIR emissions from the lanthanide ions of a Pd- or free base chlorin-appended Nd do3a complex and Yb do3a complex. Unfortunately, the characteristic NIR peaks of Yb (980 nm) and Nd (1064 nm) could not be observed at the maximum aperture of the available setup, even in deuterated solvents and in deoxygenated solutions, which means that the NIR emission should be extremely weak. In our previous work demonstrating the Yb and Nd sensitisation by chlorin chromophores, the NIR emission was faint, and required a laser excitation to be observed. Further studies with an instrumentation optimised for NIR emissions would be required to assess the potential of these dyads as NIR emitters. In parallel, solid state measurements could provide valuable results. Lanthanide complexes are usually stronger emitters in solid state than in solution.

Conclusions

The de novo synthesis of a set of hydroporphyrins (chlorins) with various reactive groups (COOH, azide, alkyne) were prepared. Such bioconjugatable red-absorbing chromophores could be useful for targeted photodynamic therapy or fluorescence imaging. Attachment of the chlorins to lanthanide complexes was achieved using either a three-step ligand coupling-deprotection-Ln-complexation protocol, or CuAAC

with pre-formed lanthanide complexes. The photophysics of the chlorin reference compounds were well characterised and were promising. However, once appended to NIR-emitting lanthanides, no NIR sensitisation could be observed. The linker in this type of chlorin-lanthanide dyads was found to be crucial for the photophysical properties, and probably also plays a significant role in outlining aggregation. The poor solubility of these structures is indeed a major issue that should be considered when designing such molecular tools. Therefore, derivatisations of the chlorin moiety with solubilising groups or linkers[54, 55] using the same chemistry developed here could transform these molecules into valuable probes. It is worth noting that even in this limited set of compounds, very small overlap between the Q-band absorption of the different compounds, as well as between their emission bands is achievable by simple metallation, suggesting that multicolour excitation spectroscopy is a possibility with suitable instrumentation. Finally, an investigation of the chlorin moieties for singlet oxygen production provides an interesting avenue for PDT-applications.

Experimental

General Procedures

^{1}H NMR (300 MHz, 400 MHz or 500 MHz) and ^{13}C NMR (75 MHz, 100 MHz or 125 MHz) spectra were recorded on a Varian 300, a Varian 400 or a Bruker 500 MHz instrument, respectively. Chemical shifts were referenced to residual solvent peaks and are given as follows: chemical shift (δ, ppm), multiplicity (s, singlet; br, broad singlet; d, doublet; t, triplet; q, quartet; m, multiplet), coupling constant (Hz), integration. IR experiments were performed on a Perkin Elmer Spectrum-100 FT-IR spectrometer equipped with an ATR accessory. HR-ESI-MS analyses were performed on a Bruker MicroTOF ESI mass spectrometer, or by the mass spectrometry service of the Ecole Polytechnique Federale de Lausanne. Compounds **1c**,[56] **1d**,[57] **6**, **7** and **7-COOH**,[36] 2-azido *O*-tosylethanol,[58] and Western half[40] were synthesised as reported in the literature. Complexes **11Ln**,[46] **12Ln**,[48] and ligand **10**[20] were prepared analogously to known compounds. All other chemicals were from commercial sources and used as received. Microwave heating was performed with a Biotage Initiator instrument.

Chromatography

Preparative chromatography was performed using silica (230–400 mesh). Thin layer chromatography was performed on silica-coated aluminium plates. Samples were visualised by UV-light (254 and 356 nm), or by staining with $KMnO_4/K_2CO_3$. RP-HPLC was performed on an Agilent Technologies 1100 system using a Chromolith® Performance RP-18 end-capped 100 mm*4.6 mm HPLC column with water (0.1% TFA) : CH_3CN (0.1% TFA) eluent system (0 min: 100% water; 8 min: 100 % CH_3CN; 10 min: 100% CH_3CN; 0 min: 100% water). Detection wavelengths: 214, 254, 397, 596 nm.

Photophysical measurements

All measurements were performed in spectroscopic grade solvents. Quartz cells with 1 cm or 0.2 cm optical pathlengths were used for the room temperature measurements. The absorbances were measured by a Varian Cary 100 Bio UV-Visible spectrophotometer. The emission and excitation spectra, lifetimes and quantum yields were measured by a FluoroMax-4P from Horiba. NIR measurements were attempted on a

Fluorolog-3 from Horiba equipped with a red sensitive PMT spanning the 400-1100 nm spectral range. All emissions were corrected by the wavelength sensitivity (correction function) of the spectrometer. The quantum yields were measured at room temperature and relative to fluorescence grade tetraphenylporphyrin (TPP). A 1 μM concentration solution of TPP in toluene was used as a quantum yield standard, Φ_f = 11%. The quantum yields were calculated according to eq(1), with Φ_s the quantum yield of the sample, Φ_{ref} the quantum yield of the reference, I the integrated corrected emission intensity of the sample (s) and of the reference (ref), A the absorptance ($\neq$ absorbance) of the sample (s) and of the reference (ref) at the excitation wavelength and n the refractive indexes of the sample (s) and of the reference (ref). Excitation wavelengths where the absorptances of the samples and of the reference were the same were chosen (i.e. where the absorptions are identical, so are the absorptances). The low temperature measurements were done in quartz capillaries at 77 K by immersion in a quartz Dewar filled with liquid nitrogen.

$$\Phi_s = \frac{I_s}{I_{ref}} \cdot \frac{A_{ref}}{A_s} \cdot \frac{(n_s)^2}{(n_{ref})^2} \cdot \Phi_{ref}$$

eq(1)

SYNTHESIS

General procedure for dipyrromethane synthesis. Following a previously reported procedure,[59] the aldehyde (1 equiv.) was dissolved in pyrrole (20 equiv.), and InCl₃ (0.1 equiv.) was added to this solution. The reaction mixture was stirred at room temperature under a nitrogen atmosphere for ~ 3 h. When TLC-analysis (petroleum ether:EtOAc:CH₂Cl₂ = 7:1:2) indicated the disappearance of the aldehyde, powdered NaOH (0.5 equiv.) was added. Stirring was continued for an additional 15 min. The mixture was filtered, the filter cake was washed with a small amount of CH₂Cl₂, and the filtrate was concentrated under reduced pressure. The dark oily residue was purified by column chromatography [silica, petroleum ether:EtOAc:CH₂Cl₂ (7:1:2)] to afford the dipyrromethanes.

2a. Brown oil (83%): t_R 3.909 min; ν_{max} 3372, 2931, 2871, 2103, 1608, 1557, 1508, 1459, 1300, 1237, 1174, 1090, 1026 cm⁻¹; ¹H NMR (300 MHz, CDCl₃) 3.59 (t, J = 4.8 Hz, 2H), 4.15 (t, J = 4.8 Hz, 2H), 5.40 (s, 1H), 5.94 (d, J = 0.6 Hz, 2H), 6.20–6.22 (m, 2H), 6.67–6.68 (m, 2H), 6.91, 7.16 (ABq, J = 8.6 Hz, 4H), 7.88 (br, 1H); ¹³C NMR (75 MHz, CDCl₃) 43.2, 50.2, 67.1, 107.2, 108.4, 114.7, 117.3, 129.6, 132.9, 135.1, 157.2; HR-ESI-MS calcd 306.1360 obsd 306.1350 [(M − H)⁻, M = C₁₇H₁₇N₅O].

2b. Off-white solid (62%): t_R 3.743 min; ν_{max} 3381, 3289, 2923, 2120, 1606, 1507, 1215, 1176, 1113, 1089, 1025 cm⁻¹; ¹H NMR (400 MHz, CDCl₃) 2.51 (s, 1H), 4.68 (s, 2H), 5.44 (s, 1H), 5.91 (s, 2H), 6.16 (d, J = 2.4 Hz, 2H), 6.70 (s, 2H), 6.93 (d, J = 8.2 Hz, 2H), 7.15 (d, J = 8.2 Hz, 2H), 7.91 (br, 2H); ¹³C NMR (100 MHz, CDCl₃) 43.2, 55.9, 75.6, 78.6, 107.2, 108.4, 115.0, 117.2, 129.4, 132.7, 135.2, 156.5; HR-ESI-MS calcd 275.1200 obsd 275.1190 [(M − H)⁻, M = C₁₈H₁₆N₂O].

2c. Pale brown solid (70%): t_R 3.734 min; ν_{max} 3372, 3100, 2409, 2115, 1678, 1502, 1283, 1114, 1089, 1027 cm⁻¹; ¹H NMR (400 MHz, THF-d_8) 5.37 (s, 1H), 5.64 (s, 1H), 5.94 (d, J = 4.0 Hz, 2H), 6.60 (d, J = 4.0 Hz, 2H), 6.96, 7.19 (ABq, J = 10.0 Hz, 4H), 9.71 (br, 1H); ¹³C NMR (100 MHz, THF-d_8) 43.6, 106.7, 107.0, 116.7, 118.4, 129.8, 132.7, 137.9, 140.9; HR-APPI-MS calcd 263.1165 obsd 263.1170 [M⁺, M = C₁₅H₁₃N₅].

2d. Yellow oil (99%): t_R 6.223 min; ν_{max} 3378, 2943, 2865, 2155, 1679, 1557, 1506, 1463, 1404, 1221, 1090, 1028 cm⁻¹; ¹H NMR (400 MHz, THF-d_8) 1.15–1.21 (m, 21H), 5.38 (s, 1H), 5.66 (s, 2H), 5.93–5.94 (m, 2H), 6.59 (s, 2H), 7.16, 7.35 (ABq, J = 8.0 Hz, 4H), 9.70 (br, 2H); ¹³C NMR (100 MHz, THF-d_8) 11.3, 18.1, 44.1, 88.7, 106.7, 107.0, 107.7, 116.8, 121.1, 128.4, 131.4, 132.4, 144.5; HR-ESI-MS calcd 401.2418 obsd 401.2421 [(M − H)⁻, M = C₂₆H₃₄N₂Si].

General synthesis of monoformyl-dipyrromethanes. A solution of the dipyrromethane in anhydrous CH₂Cl₂ [0.1 M after addition of (COCl)₂] was cooled in an ice-water bath under a nitrogen atmosphere. This solution was treated with the Vilsmeier reagent formed from (COCl)₂ (1.2 equiv.) and DMF (0.5 mL) at 0 °C. The reaction was monitored by TLC analysis [petroleum ether:EtOAc (3:1)], if required an additional portion (0.5 equiv.) of the Vilsmeier reagent was added after 30 min. When TLC analysis indicated the consumption of the starting material and the formation of a major, more polar compound, aqueous NaOH was added. The phases were separated, and the aqueous layer was extracted with CH₂Cl₂. The combined organic layer was washed with water and brine, and was dried (Na₂SO₄). The solvent was evaporated and the oily residue was purified by column chromatography [silica, petroleum ether:EtOAc (3:1→2:1)].

3a. Brown, slowly solidifying oil (55%): t_R 3.741 min; ν_{max} 3250, 2931, 2869, 2105, 1631, 1561, 1508, 1485, 1412, 1350, 1300, 1236, 1173, 1040 cm⁻¹; ¹H NMR (300 MHz, CDCl₃) 3.58 (t, J = 4.8 Hz, 2H), 4.11 (t, J = 4.8 Hz, 2H), 5.48 (s, 1H), 5.92–5.95 (m, 1H), 6.08–6.11 (m, 1H), 6.13–6.16 (m, 1H), 6.70–6.72 (m, 1H), 6.81–6.89 (m, 3H), 7.06–7.10 (m, 2H), 8.31 (br, 1H), 9.21 (d, J = 2.1 Hz, 1H), 9.76 (br, 1H); ¹³C NMR (75 MHz, CDCl₃) 43.3, 51.1, 67.0, 107.7, 108.5, 110.8, 114.8, 117.9, 122.6, 129.5, 130.8, 132.2, 133.4, 143.3, 157.5, 178.7; HR-ESI-MS calcd 334.1280 obsd 334.1309 [(M − H)⁻, M = C₁₈H₁₇N₅O₂].

3b. Brownish oil (42%): t_R 3.583 min; ν_{max} 3281, 2825, 2120, 1634, 1507, 1485, 1413, 1351, 1302, 1262, 1216, 1175, 1025 cm⁻¹; ¹H NMR (300 MHz, CDCl₃) 2.52 (t, J = 2.2 Hz, 1H), 4.67 (d, J = 2.2 Hz, 2H), 5.47 (s, 1H), 5.94 (s, 1H), 6.08–6.10 (m, 1H), 6.14–6.17 (m, 1H), 6.70–6.72 (m, 1H), 6.87–6.93 (m, 3H), 7.10 (d, J = 8.7 Hz, 2H), 8.17 (br, 1H), 9.25 (s, 1H), 9.48 (br, 1H); ¹³C NMR (75 MHz, CDCl₃) 43.3, 55.8, 75.7, 78.5, 107.8, 108.6, 110.8, 115.0, 115.2, 117.9, 122.3, 129.4, 130.7, 132.2, 133.5, 143.0, 156.8, 178.7; HR-ESI-MS calcd 303.1139 obsd 303.1079 [(M − H)⁻, M = C₁₉H₁₆N₂O₂].

3c. Brown solid (38%): t_R 3.734 min; ν_{max} 3244, 2921, 2854, 2122, 1640, 1504, 1484, 1412, 1348, 1286, 1178, 1044 cm⁻¹; ¹H NMR (300 MHz, CDCl₃) 5.52 (m, 1H), 6.09–6.11 (m, 1H), 6.14–6.16 (m, 1H), 6.71–6.73 (m, 1H), 6.89–6.96 (m, 3H), 7.12–7.16 (m, 2H), 8.33 (br, 1H), 9.24 (d, J = 1.2 Hz, 1H), 9.87 (br, 1H); ¹³C NMR (75 MHz, CDCl₃) 43.5, 108.0, 108.6, 110.9, 118.1, 119.3, 122.6, 129.7, 130.3, 132.4, 137.4, 139.2, 142.8, 178.8; HR-ESI-MS calcd 314.1012 obsd 314.1013 [(M + Na)⁺, M = C₁₆H₁₃N₅O].

3d. Brown oil (88%): t_R 6.068 min; ν_{max} 3253, 2942, 2864, 2154, 1630, 1560, 1487, 1463, 1413, 1350, 1220, 1177, 1042, 1018, 996 cm⁻¹; ¹H NMR (300 MHz, CDCl₃) 1.05–1.16 (m, 21H), 5.51 (s, 1H), 5.94–5.97 (m, 1H), 6.07–6.09 (m, 1H), 6.16 (dd, J_1 = 6.0 Hz, J_2 = 2.4 Hz, 1H), 6.71–6.74 (m, 1H), 6.88–6.90 (m, 1H), 7.08–7.10 (m, 2H), 7.39–7.43 (m, 2H), 8.21 (br, 1H), 9.24 (s, 1H), 9.58 (br, 1H); ¹³C NMR (75 MHz, CDCl₃) 11.3, 18.7, 43.9, 91.2, 106.5, 108.1, 108.7, 110.9, 118.1, 122.4, 122.8, 128.2, 130.0, 132.4, 132.5, 140.7, 142.2, 178.7; HR-ESI-

MS calcd 431.2526 obsd 431.2513 [(M + H)$^+$, M = C$_{27}$H$_{34}$N$_2$OSi].

General procedure for chlorin formation. Based on the procedure developed for sparsely substituted chlorins.[39] A solution of the formyldipyrromethane (0.1 M in THF) was cooled in an acetone-dry ice bath. A single portion of NBS (1.05 equiv.) was added, and the reaction mixture was stirred for 1 h. The cooling bath was removed, and the mixture was diluted with sat. aq. NaHCO$_3$ and EtOAc. The phases were separated. The aqueous layer was extracted with EtOAc, and the combined organic layers were dried (Na$_2$SO$_4$). The organic layer was concentrated under reduced pressure without heating. The dark brown, oily residue was used in the condensation step without further purification. The Eastern half and the Western half[40] (1 equiv.) were dissolved in CH$_2$Cl$_2$ (0.05 M), and the solution was placed under a N$_2$ atmosphere. A solution of *p*-TsOH·H$_2$O (5 equiv.) in MeOH (1 M) was added dropwise. Stirring was continued for 30 min. The reaction was quenched by the addition of tetramethylpiperidine (TMPi, 10 equiv.), and the mixture was concentrated under reduced pressure without heating. The dark yellow solid thus obtained was dissolved in CH$_3$CN (0.005 M). TMPi (25 equiv.), Zn(OAc)$_2$ (15 equiv.), and finally AgOTf (3 equiv.) were added, and the flask was placed into a bath pre-heated to 85 °C. The mixture was heated open to the air for 18–24 h. When TLC analysis (silica, CH$_2$Cl$_2$) indicated that chlorin formation was complete, the mixture was concentrated, and briefly dried to remove high-polarity solvent residues. The crude product was loaded onto a silica chromatography column, and the chlorin, a dark green apolar band, was isolated by elution with CH$_2$Cl$_2$/petroleum ether.

5a. Green solid (37%): t$_R$ 5.572 min; ν$_{max}$ 2955, 2927, 2107, 1610, 1575, 1523, 1508, 1236, 1175, 1005 cm^{-1}; ^{1}H NMR (400 MHz, CDCl$_3$/CD$_3$OD) 2.00 (s, 6H), 3.42 (t, *J* = 4.8 Hz, 2H), 4.04 (t, *J* = 4.8 Hz, 2H), 4.46 (s, 2H), 7.06 (d, J = 8.4 Hz, 2H), 7.95 (d, *J* = 8.4 Hz, 2H), 8.49 (d, *J* = 4.0 Hz, 1H), 8.54 (s, 1H), 8.58–8.59 (m, 2H), 8.65 (d, *J* = 4.4 Hz, 1H), 8.73 (d, *J* = 4.4 Hz, 1H), 8.83 (d, *J* = 4.0 Hz, 1H), 9.03 (d, *J* = 4.0 Hz, 1H), 9.56 (s, 1H); ^{13}C NMR (400 MHz, CDCl$_3$/CD$_3$OD) 34.8, 49.3, 54.2, 54.4, 71.0, 97.3, 100.1, 112.7, 116.5, 126.5, 130.5, 131.1, 131.6, 132.5, 136.5, 138.7, 140.1, 149.95, 150.0, 150.2, 151.3, 156.9, 157.8, 161.6, 162.8, 174.8. HR-ESI-MS calcd 564.1494 obsd 564.1485 [(M + H)$^+$, M = C$_{30}$H$_{25}$N$_7$OZn].

5b. Bluish-green solid (50%): t$_R$ 5.444 min; ν$_{max}$ 3293, 2957, 1617, 1508, 1218, 1176, 1052, 1007, 992 cm^{-1}; ^{1}H NMR (400 MHz, CDCl$_3$/CD$_3$OD) 2.00 (s, 6H), 2.67 (s, 1H), 4.46 (s, 2H), 4.88 (s, 2H), 7.27 (d, *J* = 8.8 Hz, 2H), 8.02 (d, *J* = 8.0 Hz, 2H), 8.53–8.55 (m, 2H), 8.58–8.60 (m, 2H), 8.69 (d, *J* = 4.4 Hz, 1H), 8.74 (d, *J* = 4.4 Hz, 1H), 8.84 (d, *J* = 4.4 Hz, 1H), 9.04 (d, *J* = 4.4 Hz, 1H), 9.56 (s, 1H); ^{13}C NMR (100 MHz, CDCl$_3$/CD$_3$OD) 31.0, 45.4, 50.4, 75.8, 78.8, 93.4, 96.2, 108.7, 113.0, 122.5, 126.6, 127.2, 127.7, 128.6, 132.5, 132.7, 134.7, 136.4, 146.0, 146.3, 152.9, 153.9, 157.0, 158.8, 170.8; HR-ESI-MS calcd 532.1236 obsd 532.1248 [M$^+$, M = C$_{31}$H$_{24}$N$_4$OZn].

5c. Green solid (23%): t$_R$ 5.742 min; ν$_{max}$ 3034, 2956, 2923, 2410, 2253, 2120, 2086, 1614, 1523, 1503, 1300, 1269, 1180, 1143, 1049, 1005 cm^{-1}; ^{1}H NMR (400 MHz, CDCl$_3$) 2.02 (s, 6H), 4.52 (s, 2H), 7.34 (d, *J* = 7.8 Hz, 2H), 8.06 (d, *J* = 7.8 Hz, 2H), 8.47 (d, *J* = 3.9 Hz, 1H), 8.56 (s, 1H), 8.62–8.64 (m, 3H), 8.75 (d, *J* = 3.9 Hz, 1H9, 8.85 (d, *J* = 3.9 Hz, 1H), 9.06 (d, *J* = 3.9 Hz, 1H), 9.58 (s, 1H); ^{13}C NMR (75 MHz, CDCl$_3$) 43.3, 55.8, 75.7, 78.5, 107.8, 108.6, 110.8, 115.0, 115.2, 117.9, 122.3, 129.4, 130.7, 132.2, 133.5, 143.0, 156.8, 178.7; HR-ESI-MS calcd 519.1144 obsd 519.1164 [M$^+$, M = C$_{28}$H$_{21}$N$_7$Zn].

5d-TIPS. Green solid (12%): t$_R$ 7.679 min; ν$_{max}$ 2942, 2865, 2154, 1615, 1524, 1501, 1463, 1221, 1051, 1007, 992 cm^{-1}; ^{1}H NMR (400 MHz, CDCl$_3$/CD$_3$OD) 1.17 (s, 21H), 1.96 (s, 6H), 4.47 (br, 2H), 7.74 (d, *J* = 7.4 Hz, 2H), 7.96 (d, *J* = 7.4 Hz, 2H), 8.40 (s, 1H), 8.50 (s, 1H), 8.55 (s, 2H), 8.68 (s, 1H), 8.77 (s, 1H), 8.99 (s, 1H), 9.51 (s, 1H); ^{13}C NMR (100 MHz, CDCl$_3$/CD$_3$OD) 11.4, 18.7, 30.9, 45.3, 50.3, 91.1, 93.5, 96.2, 107.4, 108.7, 122.0, 122.2, 126.7, 127.7, 128.3, 130.1, 132.5, 133.6, 143.3, 146.0, 146.2, 146.6, 152.8, 153.8, 158.9, 170.8; HR-ESI-MS calcd 659.2543 obsd 659.2594 [(M + H)$^+$, M = C$_{39}$H$_{42}$N$_4$SiZn].

5d. A sample of **5d-TIPS** (27 mg, 0.055 mmol) in CH$_2$Cl$_2$ (2 mL) was treated with AcOH (5 μL) and TBAF[60] in THF (2 mL, 1 M). After 1 h TLC-analysis indicated the complete consumption of the starting material. Water and EtOAc were added to the reaction mixture, the phases were separated, and the organic phase was washed with water, and dried (Na$_2$SO$_4$). Column chromatography [silica, CH$_2$Cl$_2$/petroleum ether (1:1)] afforded a dark green solid (55%): t$_R$ 5.626 min; ν$_{max}$ 3288, 2954, 2922, 2854, 1610, 1521, 1498, 1445, 1262,1215, 1050, 1003 cm^{-1}; ^{1}H NMR (400 MHz, CDCl$_3$/CD$_3$OD) 1.99 (s, 6H), 2.86 (s, 1H), 4.46 (s, 2H), 7.32 (d, *J* = 7.6 Hz, 2H), 8.05 (d, *J* = 8.0 Hz, 2H), 8.46 (d, *J* = 4.4 Hz, 1H), 8.54 (s, 1H), 8.59–8.61 (m, 3H), 8.72 (d, *J* = 4.0 Hz, 1H), 8.82 (d, *J* = 4.0 Hz, 1H), 9.02 (d, *J* = 4.4 Hz, 1H), 9.55 (s, 1H); ^{13}C NMR (100 MHz, CDCl$_3$/CD$_3$OD) 31.0, 45.4, 50.4, 93.6, 96.3, 108.7, 117.1, 121.7, 126.8, 127.3, 127.8, 128.3, 132.3, 132.6, 135.0, 139.1, 139.9, 145.8, 146.0, 146.3, 146.9, 152.9, 153.9, 159.0, 170.9. HR-ESI-MS calcd 503.1136 obsd 503-1209 [(M + H)$^+$, M = C$_{30}$H$_{22}$N$_4$Zn].

8Pd. Following the procedure developed by Bruckner,[42] a microwave vial was charged with **7** (47 mg, 0.086 mmol) and Pd(acac)$_2$ (131 mg, 0.43 mmol, 5 equiv.). Pyridine (6 mL) was added, the vial was capped, and the mixture was heated at 180 °C for 30 min with microwave irradiation. The mixture was concentrated, and the residue was purified by column chromatography [silica, pentane/CH$_2$Cl$_2$ (1:2)]. A pink solid was obtained (63%): t$_R$ 6.669 min; ν$_{max}$ 2961, 2926, 1748, 1626, 1509, 1259, 1215, 1150, 1079, 1006 cm^{-1}; ^{1}H NMR (400 MHz, CDCl$_3$/CD$_3$OD) 1.55 (s, 9H), 1.94 (s, 6H), 4.50 (s, 2H), 4.72 (s, 2H), 7.16 (d, *J* = 8.4 Hz, 2H), 7.89 (d, J = 8.4 Hz, 2H), 8.47 (d, *J* = 4.4 Hz, 1H), 8.50 (s, 1H), 8.62 (s, 1H), 8.64 (d, *J* = 4.4 Hz, 1H), 8.77 (d, *J* = 4.0 Hz, 1H), 8.88 (d, J = 4.4 Hz, 1H), 9.61 (s, 1H); ^{13}C NMR (100 MHz, CDCl$_3$/CD$_3$OD) 24.1, 26.7, 41.5, 62.0, 78.8, 105.9, 109.0, 122.3, 123.0, 123.3, 127.9, 128.0, 130.4, 130.7, 153.7, 164.5; HR-APPI-MS calcd 651.1595 obsd 651.1697 [(M + H)$^+$, M = C$_{34}$H$_{32}$N$_4$O$_3$Pd].

8Ni. A microwave vial was charged with **7** (27 mg, 0.049 mmol) and Ni(OAc)$_2$·4H$_2$O (122 mg, 0.49 mmol, 10 equiv.). Pyridine (3 mL) was added, the vial was capped, and the mixture was heated at 180 °C for 30 min with microwave irradiation. The mixture was concentrated, and the residue purified by column chromatography [silica, pentane/CH$_2$Cl$_2$ (1:2)]. A reddish green solid was obtained (68%): t$_R$ 6.616 min; ν$_{max}$ 2960, 2927, 1752, 1642, 1511, 1368, 1217 cm^{-1}; ^{1}H NMR (400 MHz, CDCl$_3$) 1.59 (s, 9H), 1.81 (s, 6H), 4.13 (br, 2H), 4.74 (s, 2H), 7.17 (d, *J* = 7.8 Hz, 2H), 7.82 (d, *J* = 7.8 Hz, 2H), 8.14 (s, 1H), 8.23 (s, 1H), 8.32–8.34 (m, 2H), 8.47–8.48 (m, 2H), 8.60 (d, *J* = 4.3 Hz, 1H), 8.78 (d, *J* = 4.3 Hz, 1H), 9.21 (s, 1H); ^{13}C NMR (100 MHz, CDCl$_3$) 28.2, 45.8, 50.2, 66.0, 82.5, 93.5, 96.2, 113.2, 126.7, 127.4, 128.0, 128.5, 133.0, 133.1, 133.8, 134.0, 157.7, 168.1; HR-APPI-MS calcd 603.1901 obsd 603.1910 [(M + H)$^+$, M = C$_{34}$H$_{32}$N$_4$O$_3$Ni].

8Cu. A solution of **7** (50 mg, 0.1 mmol) in CHCl$_3$/MeOH (9:1, 20 mL) was treated with Cu(OAc)$_2$·H$_2$O (10 equiv.). The mixture was stirred at room temperature overnight. The sample was diluted with water and CH$_2$Cl$_2$, the phases were separated, and the aqueous layer was extracted with CH$_2$Cl$_2$. The combined organic layer was washed with water, dried (Na$_2$SO$_4$) and concentrated. The residue purified by column chromatography [silica, pentance/CH$_2$Cl$_2$ (1:2)] affording a dark blue-green solid (58%): t$_R$ 6.910 min; ν_{max} 2957, 1750, 1639, 1602, 1539,1515, 1380, 1366, 1326, 1215, 1151, 1054, 1006 cm^{-1}; HR-ESI-MS calcd 607.1765 obsd 607.1768 [M$^+$, M = C$_{34}$H$_{32}$CuN$_4$O$_3$].

9Pd. Following the procedure developed by Bruckner,[42] a microwave vial was charged with **7-COOH** (19 mg, 0.038 mmol) and Pd(acac)$_2$ (236 mg, 0.775 mmol). Pyridine (4 mL) was added, the vial was capped, and the mixture was heated at 180 °C for 30 min with microwave irradiation. The mixture was concentrated, and the residue was purified by column chromatography [silica, CH$_2$Cl$_2$/MeOH (20:1→10:1)]. A pink solid was obtained (70%): t$_R$ 5.596 min; ν_{max} 2923, 2854, 1740, 1635, 1604, 1510, 1427, 1362, 1328, 1228, 1214, 1177, 1059, 1009 cm^{-1}; ^{1}H NMR (400 MHz, CD$_3$OD/CDCl$_3$) 1.94 (s, 6H), 4.48 (s, 2H), 4.86 (s, 2H), 7.23 (d, J = 8.2 Hz, 2H), 7.88 (d, J = 8.2 Hz, 2H), 8.45 (d, J = 4.3 Hz, 1H), 8.49 (s, 2H), 8.64–8.67 (m, 3H), 8.76 (d, J = 4.3 Hz, 1H), 8.89 (d, J = 4.7 Hz, 1H), 9.60 (s, 1H); ^{13}C NMR (100 MHz, CD$_3$OD/CDCl$_3$) 30.2, 45.2, 49.7, 65.1, 95.1, 97.5, 109.7, 112.9, 123.3, 126.2, 126.9, 127.1, 127.4, 131.7, 134.3, 134.6, 137.3, 137.5, 138.3, 138.8, 142.0, 144.6, 145.5, 149.9, 157.7, 161.6, 171.4; HR-ESI-MS calcd 593.0822 obsd 593.0979 [(M – H)$^-$, M = C$_{30}$H$_{24}$N$_4$O$_3$Pd].

9Ni. **Procedure 1.** A microwave vial was charged with **8Ni** (20 mg, 0.040 mmol). Benzonitrile (2 mL) was added, the vial was capped, and the mixture was heated at 210 °C for 30 min with microwave irradiation. The mixture was concentrated, and the residue purified by column chromatography [silica, CH$_2$Cl$_2$/MeOH (20:1→10:1)]. A dark green solid was obtained (83%).

Prodecure 2. A microwave vial was charged with **7-COOH** (30 mg, 0.061 mmol) and Ni(OAc)$_2$·H$_2$O (152 mg, 0.61 mmol, 10 equiv.). Pyridine (3 mL) was added, the vial was capped, and the mixture was heated at 180 °C for 30 min with microwave irradiation. The mixture was concentrated, and the residue was purified by column chromatography [silica, CH$_2$Cl$_2$/MeOH (20:1→10:1)]. A dark green solid was obtained (81%): t$_R$ 5.557 min; ν_{max} 2922, 1611, 1509, 1456, 1380, 1317, 1238, 11176, 1051, 1003, 988 cm^{-1}; ^{1}H NMR (400 MHz, CD$_3$OD/CDCl$_3$) 1.74 (s, 6H), 3.96 (s, 2H), 4.75 (s, 2H), 7.19 (d, J = 7.9 Hz, 2H), 7.74 (d, J = 7.9 Hz, 2H), 8.04 (s, 1H), 8.12 (s, 1H), 8.17 (s, 1H), 8.23 (d, J = 4.0 Hz, 1H), 8.34 (d, J = 4.3 Hz, 1H), 8.44 (d, J = 3.9 Hz, 1H), 8.50 (d, J = 3.9 Hz, 1H), 8.73 (d, J = 4.3 Hz, 1H), 9.14 (s, 1H); ^{13}C NMR (100 MHz, CD$_3$OD/CDCl$_3$) 19.9, 27.7, 45.4, 49.7, 64.9, 93.2, 95.9, 108.2, 112.9, 124.3, 126.5, 127.2, 127.9, 130.5, 132.8, 133.8, 157.7, 171.4, 174.0; HR-ESI-MS calcd 545.1129 obsd 545.1169 [(M – H)$^-$, M = C$_{30}$H$_{23}$N$_2$NiO$_3$].

9Cu. A solution of **7-COOH** (5 mg, 0.010 mmol) in CH$_2$Cl$_2$/MeOH (3:1, 4 mL) was treated with Cu(OAc)$_2$·H$_2$O (10 equiv.). The mixture was stirred at room temperature for 5 min. The sample was concentrated, and the residue was purified by column chromatography [silica, CH$_2$Cl$_2$/MeOH (20:1)] affording a green solid (85%): t$_R$ 5.787 min; ν_{max} 2921, 2852, 1639, 1602, 1464, 1424, 1226, 1053, 1007, 994 cm^{-1}; HR-ESI-MS calcd 550.1072 obsd 550.1090 [(M – H)$^-$, M = C$_{30}$H$_{24}$CuN$_4$O$_3$].

General procedure for amide bond formation. The chlorin carboxylic acid (1 equiv.) and the amine-functionalised cyclen (1.1 mmol) were dissolved in anhydrous DMF (0.024 M). The solution was cooled in an ice-water bath, and DIPEA (2.2 equiv.) and HATU (1.1 mmol) were added. The reaction was allowed to warm to room temperature, and stirring was continued for ~24–48 h. When TLC analysis indicated the complete consumption of the starting chlorin, the reaction mixture was diluted with EtOAc and dil. aq. NaHCO$_3$. The phases were separated, and the aqueous layer was extracted with EtOAc. The combined organic phases were washed with water twice, and dried (Na$_2$SO$_4$). The organic layer was concentrated, and the oily residue was purified by column chromatography [silica, CH$_2$Cl$_2$/MeOH (20:1→10:1)].

13Pd. Pink solid (93%): t$_R$ 5.277 min; ν_{max} 2958, 2842, 1732, 1510, 1441, 1311, 1221, 1173, 1113, 1009 cm^{-1}; ^{1}H NMR (400 MHz, CDCl$_3$/CD$_3$OD) Multiple conformers were seen, peaks are reported for all of them. Due to solvent overlap and uncertainties in integration, integral values are only reported for the 4.49–9.59 ppm region. 1.17–3.80 (m), 1.93 (s), 4.49 (s, 1.74H), 4.61 (s, 1.16H), 7.22–7.23 (m, 1.74H), 7.51 (m, 0.35H), 7.77–7.88 (m, 3.19H), 8.21–8.23 (m, 0.43H), 8.41–8.49 (m, 2.83H), 8.58 (m, 0.62H), 8.63 (s, 1.85H), 8.69 (s, 1H), 8.74 (s, 1H), 8.87 (s, 1H), 9.59 (s, 1H); HR-ESI-MS calcd 1008.3611 obsd 1008.3627 [(M + H)$^+$, M = C$_{49}$H$_{59}$N$_9$O$_8$Pd].

13Cu. Bluish-green solid (92%): t$_R$ 5.414 min; ν_{max} 3412, 2957, 2834, 1730, 1641, 1516, 1441, 1381, 1310, 1219, 1178, 1112, 993 cm^{-1}; HR-ESI-MS calcd 965.4193 obsd 965.3855 [(M + H)$^+$, M = C$_{49}$H$_{59}$CuN$_9$O$_8$].

13Ni. Dark green solid (65%): t$_R$ 5.906 min; ν_{max} 2925, 1735, 1649, 1439, 1381, 1211, 1170, 996; ^{1}H NMR (400 MHz, CDCl$_3$) Multiple conformers were seen, peaks are reported for all of them. Even after extensive purification and drying ~1 molecule of DMF was retained. Due to solvent overlap and uncertainties in integration, integral values are only reported for the 4.09–9.17 ppm region. 1.20–3.77 [m, contains 1.75 (s, 6H)] 4.09 (s, 2H), 4.63 (s, 2H), 7.18 (d, J = 7.8 Hz, 2H), 7.40–7.41 (m, 0.51H), 7.46–4.74 (m, 1H), 7.74–7.78 (m, 2.5 H), 7.93 (s, 1.25H, DMF), 8.12 (s, 1H), 8.20 (as, 3H), 8.29 (d, J = 4.3 Hz, 1H), 8.36 (d, J = 4.7 Hz, 1H), 8.43 (d, J = 4.3 Hz, 1H), 8.54 (d, J = 4.3 Hz, 1H), 8.74 (d, J = 4.3 Hz, 1H), 9.17 (s, 1H).

General procedure for methyl ester deprotection. A sample of the protected ligand (0.028 mmol) was dissolved in THF (0.5 mL). 1 M LiOH (aq, 0.5 mL), 1 M NaOH (aq, 0.5 mL) and 1 M KOH (aq, 0.5 mL) were added, and the reaction mixture was heated at 70 °C for 2–3 days. The reaction progress was monitored by RP-HPLC. If deemed necessary, additional portions of LiOH or KOH were added. When RP-HPLC analysis indicated the complete consumption of the starting material, the reaction mixture was concentrated, and the residue was purified by column chromatography [silica, CH$_2$Cl$_2$/MeOH (10:1→5:1)].

14Pd. Pink solid (26%): t$_R$ 5.577 min; ν_{max} 3341, 2949, 2837, 1453, 1018, 844 cm^{-1}; ^{1}H NMR (400 MHz, THF-d_8) 1.91 (s, 6H), 1.91–3.37 (~23H), 4.53 (s, 2H), 4.77 (s, 2H), 7.17 (d, J = 8.0 Hz, 2H), 7.82 (d, J = 8.0 Hz, 2H), 8.40 (d, J = 3.7 Hz, 1H), 8.44 (d, J = 4.7 Hz, 1H), 8.49 (d, J = 4.3 Hz, 1H), 8.63 (d, J = 4.7 Hz, 1H), 8.69–8.74 (m, 3H), 8.87 (d, J = 4.7 Hz, 1H), 9.63 (s, 1H); ^{13}C NMR (100 MHz, CDCl$_3$/THF-d_8) 13.4, 19.9, 22.4, 27.7, 29.4, 29.7, 31.7, 45.4, 49.7, 64.9, 93.2, 95.9, 108.2, 112.9, 126.5, 127.2, 127.7, 127.9, 132.5, 132.7, 133.8, 157.7, 174.0; HR-MALDI-MS calcd 966.3141 obsd 966.2492 [(M + H)$^+$, M = C$_{46}$H$_{53}$N$_9$O$_8$Pd].

14Cu. Dark blue solid (23%): t_R 5.792 min; ν_{max} 3676, 2972, 2902, 2342, 2326, 1641, 1394, 1229, 1063 cm^{-1}; HR-MALDI-MS calcd 922.3308 obsd 922.5175 (M$^+$, M = C$_{46}$H$_{53}$CuN$_9$O$_8$).

14Ni. Dark green solid (20%): t_R 6.190 min; ν_{max} 3678, 2988, 2901, 2357, 2342, 2326, 1406, 1394, 1250, 1057 cm^{-1}; ^{1}H NMR (500 MHz, THF-d_8) Due to solvent overlap with cyclen-CH_2, C(O)NHCH_2 and CH_2CO$_2$H signals, integral values are only reported for the 4.13–9.24 ppm region. 4.13 (br, 2H), 4.82 (br, 2H), 5.49–5.54 (m, 1H), 7.23 (br, 2.80H), 7.42 (br, 0.5H), 7.78 (br, 2.44H), 8.24–8.29 (m, 4H), 8.43–8.58 (m, 3H), 8.79 (br, 1H), 9.24 (br, 1H); HR-ESI-MS calcd 918.3443 obsd 918.3489 [(M + H)$^+$, M = C$_{46}$H$_{53}$N$_9$NiO$_8$].

General procedure for lanthanide complexation. A sample of the unprotected ligand (1 equiv.) and the appropriate lanthanide chloride (1.1 equiv.) were dissolved in MeOH (2 mL). The reaction mixture was heated at 70 °C, and monitored by RP-HPLC. When necessary, an additional portion of LnCl$_3$ was added (up to 10 equiv.). When RP-HPLC-analysis indicated the complete consumption of the free ligand, or the stopping of the reaction despite the addition of further portions of lanthanide salt, the mixture was allowed to cool to room temperature. The pure product precipitated out from the reaction mixture for **15NiLn**. Complexes **15PdLn** were purified by dissolution in methanol and diethyl ether, in which the other components of the reaction mixture were not soluble.

Pd15Ln. Ln = Yb, dark pink solid (*too small quantity to be accurate*): t_R 6.134 min; ν_{max} 3338, 2947, 2836, 1450, 1016 cm^{-1}. Ln = Nd, dark pink solid (*too small quantity to be accurate*): t_R 6.136 min; ν_{max} 3339, 2947, 2836, 1449, 1020 cm^{-1}; HR-ESI-MS calcd 1103.1846 obsd 1103.1979 (M − H)$^+$ [(M + H)$^+$, M = C$_{46}$H$_{49}$N$_9$NdO$_8$Pd].

Ni15Ln. Ln = Yb, dark green solid (*quant.*): t_R 5.558 min; ν_{max} 3336, 2923, 2325, 1605, 1419, 1225, 1058, 998 cm^{-1}. Ln = Nd, dark green solid (*quant.*): t_R 5.559 min; ν_{max} 3331, 2923, 2325, 1602, 1509, 1420, 1225, 1058, 998 cm^{-1}.

General procedure for CuAAC. Procedure for 0.01 mmol of chlorin substrate. The alkyne and the azide (1 equiv. chlorin, 1.5 equiv. Ln-complex) were dissolved in DMSO (0.2 mL). TBTA^{50} (0.1 equiv.), and CuOAc (0.1 equiv.) were added dissolved in DMSO (0.2 mL), followed by NaAsc (0.5 equiv., in 15 μL H$_2$O). The reaction mixture was stirred at room temperature until TLC analysis indicated the complete consumption of the starting chlorin. The mixture was concentrated under reduced pressure, and the product was precipitated from MeOH with Et$_2$O (Ln-complexes).

ZnTNYb. Dark green solid (*quant.*): t_R 5.063 min; ν_{max} 1612, 1399, 1318, 1223, 1177, 1086, 1052, 988 cm^{-1}; HR-ESI-MS calcd 1141.2457 obsd 1141.2467 [(M + Na)$^+$, M = C$_{47}$H$_{50}$N$_{11}$O$_7$YbZn].

ZnTNLn. Ln = Gd, dark green solid (*quant.*): t_R 5.123 min; ν_{max} 3364, 2161, 1603, 1380, 1316, 1231, 1176, 1083, 1051, 989 cm^{-1}; HR-MALDI-MS calcd 1102.2417 obsd 1102.2424 (M$^+$, M = C$_{47}$H$_{50}$GdN$_{11}$O$_7$Zn). Ln = Yb, dark green solid (*quant.*): t_R 5.128 min; ν_{max} 3388, 1177, 1383, 1316, 1226, 1177, 1085, 1052 cm^{-1}. Ln = Nd, dark green solid (*quant*): t_R 5.152 min; HR-MALDI-MS calcd 1086.2256 obsd 1086.2331 (M$^+$, M = C$_{47}$H$_{50}$NdN$_{11}$O$_7$Zn).

6Yb. Dark green solid (*quant.*): t_R 5.033 min; ν_{max} 3361, 2959, 2923, 1607, 1399, 1316, 1222, 1087, 1005, 988 cm^{-1}; ESI-MS calcd 1088.2 obsd 1089.6 [M$^-$, M = C$_{46}$H$_{48}$N$_{11}$O$_6$YbZn].
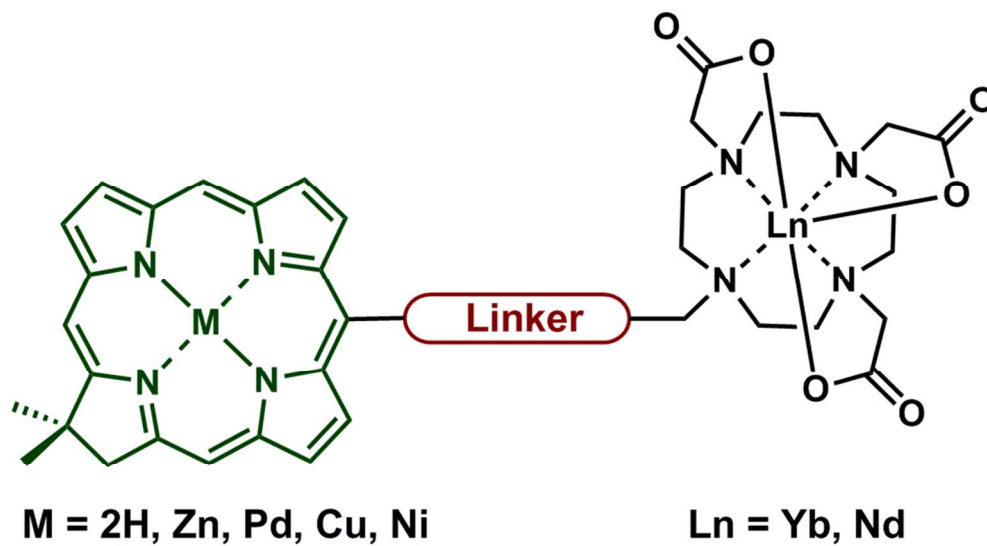
Acknowledgements

Notes and references

^{a} Department of Chemistry – BMC, Uppsala University, 75123 Uppsala, Sweden. Email: eszter.borbas@kemi.uu.se

1. S. Hampel, P. Chung, C. E. McKellar, D. Hall, L. L. Looger and J. H. Simpson, *Nat. Methods*, 2011, **8**, 253.
2. J.-C. G. Bünzli, *Chem. Rev.*, 2010, **110**, 2729.
3. D. Geißler, S. Stufler, H.-G. Löhmannsröben and N. Hildebrandt, *J. Am. Chem. Soc.*, 2012, **135**, 1102.
4. D. Geissler, S. Linden, K. Liermann, K. D. Wegner, L. J. Charbonniere and N. Hildebrandt, *Inorg. Chem.*, 2014, **53**, 1824.
5. N. Hildebrandt, K. D. Wegner and W. R. Algar, *Coord. Chem. Rev.*, 2014, **273-274**, 125.
6. E. Pershagen, J. Nordholm and K. E. Borbas, *J. Am. Chem. Soc.*, 2012, **134**, 9832.
7. M. S. Tremblay, M. Halim and D. Sames, *J. Am. Chem. Soc.*, 2007, **129**, 7570.
8. D. Parker, R. S. Dickins, H. Puschmann, C. Crossland and J. A. K. Howard, *Chem. Rev.*, 2002, **102**, 1977.
9. K. A. White, D. A. Chengelis, K. A. Gogick, J. Stehman, N. L. Rosi and S. Petoud, *J. Am. Chem. Soc.*, 2009, **131**, 18069.
10. X. Yan, L. Yang and Q. Wang, *Angew. Chem., Int. Ed.*, 2011, **50**, 5130.
11. Y. Luo, X. Yan, Y. Huang, R. Wen, Z. Li, L. Yang, C. J. Yang and Q. Wang, *Anal. Chem.*, 2013, **85**, 9428.
12. G.-L. Law, R. Pal, L. O. Palsson, D. Parker and K.-L. Wong, *Chem. Commun.*, 2009, 7321.
13. S. Faulkner, S. J. A. Pope and B. P. Burton-Pye, *Appl. Spectrosc. Rev.*, 2005, **40**, 1.
14. C. Bischof, J. Wahsner, J. Scholten, S. Trosien and M. Seitz, *J. Am. Chem. Soc.*, 2010, **132**, 14334.
15. C. Doffek, N. Alzakhem, C. Bischof, J. Wahsner, T. Gueden-Silber, J. Luegger, C. Platas-Iglesias and M. Seitz, *J. Am. Chem. Soc.*, 2012, **134**, 16413.
16. C. Doffek, N. Alzakhem, M. Molon and M. Seitz, *Inorg. Chem.*, 2012, **51**, 4539.
17. G. Mancino, A. J. Ferguson, A. Beeby, N. J. Long and T. S. Jones, *J. Am. Chem. Soc.*, 2005, **127**, 524.
18. N. Alzakhem, C. Bischof and M. Seitz, *Inorg. Chem.*, 2012, **51**, 9343.
19. M. Suchý and R. H. E. Hudson, *Eur. J. Org. Chem.*, 2008, **2008**, 4847.
20. E. Pershagen and K. E. Borbas, *Coord. Chem. Rev.*, 2014, **273-274**, 30.
21. P. Caravan, J. J. Ellison, T. J. McMurry and R. B. Lauffer, *Chem. Rev.*, 1999, **99**, 2293.
22. K. D. Daughtry, L. J. Martin, A. Sarraju, B. Imperiali and K. N. Allen, *ChemBioChem*, 2012, **13**, 2567.

Dalton Transactions Accepted Manuscript

23. N. R. Silvaggi, L. J. Martin, H. Schwalbe, B. Imperiali and K. N. Allen, *J. Am. Chem. Soc.*, 2007, **129**, 7114.

24. L. J. Martin, M. J. Haehnke, M. Nitz, J. Woehnert, N. R. Silvaggi, K. N. Allen, H. Schwalbe and B. Imperiali, *J. Am. Chem. Soc.*, 2007, **129**, 7106.

25. A. Canales, A. Mallagaray, M. A. Berbis, A. Navarro-Vazquez, G. Dominguez, F. J. Canada, S. Andre, H.-J. Gabius, J. Perez-Castells and J. Jimenez-Barbero, *J. Am. Chem. Soc.*, 2014, **136**, 8011.

26. A. Canales, A. Mallagaray, J. Perez-Castells, I. Boos, C. Unverzagt, S. Andre, H.-J. Gabius, F. J. Canada and J. Jimenez-Barbero, *Angew. Chem., Int. Ed.*, 2013, **52**, 13789.

27. D. Bini, M. Gregori, U. Cosentino, G. Moro, A. Canales, A. Capitoli, J. Jimenez-Barbero and L. Cipolla, *Carbohydr Res*, 2012, **354**, 21.

28. W.-K. Wong, X. Zhu and W.-Y. Wong, *Coord. Chem. Rev.*, 2007, **251**, 2386.

29. V. Bulach, F. Sguerra and M. W. Hosseini, *Coord. Chem. Rev.*, 2012, **256**, 1468.

30. M. Gouterman, C. D. Schumaker, T. S. Srivastava and T. Yonetani, *Chemical Physics Letters*, 1976, **40**, 456.

31. A. Beeby, R. S. Dickins, S. FitzGerald, L. J. Govenlock, C. L. Maupin, D. Parker, J. P. Riehl, G. Siligardi and J. A. G. Williams, *Chem. Commun.*, 2000, 1183.

32. E. D. Sternberg, D. Dolphin and C. Bruckner, *Tetrahedron*, 1998, **54**, 4151.

33. Borbas, K. E.; Lahaye, D. In: Photodynamic therapy of cancer, John Wiley & Sons Ltd.: 2008; pp 187-222.

34. C. P. Gros, A. Eggenspiller, A. Nonat, J.-M. Barbe and F. Denat, *MedChemComm*, 2011, **2**, 119.

35. A. Eggenspiller, C. Michelin, N. Desbois, P. Richard, J.-M. Barbe, F. Denat, C. Licona, C. Gaiddon, A. Sayeh, P. Choquet and C. P. Gros, *Eur. J. Org. Chem.*, 2013, **2013**, 6629.

36. J. Laakso, G. A. Rosser, C. Szijjarto, A. Beeby and K. E. Borbas, *Inorg Chem*, 2012, **51**, 10366.

37. Q. Wang, S.-i. Sasaki and H. Tamiaki, *Chem. Lett.*, 2009, **38**, 648.

38. J.-P. Strachan, D. F. O'Shea, T. Balasubramanian and J. S. Lindsey, *J. Org. Chem.*, 2000, **65**, 3160.

39. M. Ptaszek, B. E. McDowell, M. Taniguchi, H.-J. Kim and J. S. Lindsey, *Tetrahedron*, 2007, **63**, 3826.

40. M. Ptaszek, J. Bhaumik, H.-J. Kim, M. Taniguchi and J. S. Lindsey, *Org. Process Res. Dev.*, 2005, **9**, 651.

41. F. Bryden and R. W. Boyle, *Synlett*, 2013, **24**, 1978.

42. M. L. Dean, J. R. Schmink, N. E. Leadbeater and C. Brueckner, *Dalton Trans.*, 2008, 1341.

43. A. R. Battersby, C. J. R. Fookes and R. J. Snow, *J. Chem. Soc., Perkin Trans. 1*, 1984, 2725.

44. A. R. Battersby, K. Jones and R. J. Snow, *Angew. Chem.*, 1983, **95**, 742.

45. M. Meldal and C. W. Tornoe, *Chem. Rev.*, 2008, **108**, 2952.

46. M. Jauregui, W. S. Perry, C. Allain, L. R. Vidler, M. C. Willis, A. M. Kenwright, J. S. Snaith, G. J. Stasiuk, M. P. Lowe and S. Faulkner, *Dalton Trans.*, 2009, 6283.

47. J. K. Molloy, O. Kotova, R. D. Peacock and T. Gunnlaugsson, *Org. Biomol. Chem.*, 2012, **10**, 314.

48. C. Szijjarto, E. Pershagen and K. E. Borbas, *Dalton Trans*, 2012, **41**, 7660.

49. G. J. Stasiuk and M. P. Lowe, *Dalton Trans.*, 2009, 9725.

50. T. R. Chan, R. Hilgraf, K. B. Sharpless and V. V. Fokin, *Org. Lett.*, 2004, **6**, 2853.

51. M. Gouterman, *J. Mol. Spectrosc.*, 1961, **6**, 138.

52. C. Bruckner, J. R. McCarthy, H. W. Daniell, Z. D. Pendon, R. P. Ilagan, T. M. Francis, L. Ren, R. R. Birge and H. A. Frank, *Chem. Phys.*, 2003, **294**, 285.

53. M. Taniguchi, M. Ptaszek, B. E. McDowell, P. D. Boyle and J. S. Lindsey, *Tetrahedron*, 2007, **63**, 3850.

54. K. E. Borbas, V. Chandrashaker, C. Muthiah, H. L. Kee, D. Holten and J. S. Lindsey, *J. Org. Chem.*, 2008, **73**, 3145.

55. F. Giuntini, F. Bryden, R. Daly, E. M. Scanlan and R. W. Boyle, *Org. Biomol. Chem.*, 2014, **12**, 1203.

56. Y. Chen, A. S. Kamlet, J. B. Steinman and D. R. Liu, *Nat. Chem.*, 2011, **3**, 146.

57. J.-F. Nierengarten, S. Zhang, A. Gegout, M. Urbani, N. Armaroli, G. Marconi and Y. Rio, *J. Org. Chem.*, 2005, **70**, 7550.

58. Mach, R. H.; McConathy, J. 1H-[1, 2, 3] Triazole substituted amino acids and uses thereof. US20100278732A1, 2010.

59. J. K. Laha, S. Dhanalekshmi, M. Taniguchi, A. Ambroise and J. S. Lindsey, *Org. Process Res. Dev.*, 2003, **7**, 799.

60. A. L. Korich and T. S. Hughes, *Org. Lett.*, 2008, **10**, 5405.

Dalton Transactions Accepted Manuscript

M = 2H, Zn, Pd, Cu, Ni   Ln = Yb, Nd

89x49mm (300 x 300 DPI)